



FREE VIBRATION OF A PARTIALLY LIQUID-FILLED AND SUBMERGED, HORIZONTAL CYLINDRICAL SHELL

A. ERGIN

Faculty of Naval Architecture and Ocean Engineering, Istanbul Technical University, Maslak, 80626 Istanbul, Turkey. E-mail: ergina@itu.edu.tr

AND

P. TEMAREL

Ship Science, School of Engineering Sciences, University of Southampton, Southampton, SO17 1BJ, England

(Received 21 May 2001, and in final form 18 October 2001)

The dynamic characteristics (i.e., natural frequencies and mode shapes) of a partially filled and/or submerged, horizontal cylindrical shell are examined. In this investigation, it is assumed that the fluid is ideal, and fluid forces are associated with inertial effects only: namely, the fluid pressure on the wetted surface of the structure is in phase with the structural acceleration. The *in vacuo* dynamic characteristics of the cylindrical shell are obtained using standard finite element software. In the “wet” part of the analysis, it is assumed that the shell structure preserves its *in vacuo* mode shapes when in contact with the contained and/or surrounding fluid and that each mode shape gives rise to a corresponding surface pressure distribution of the shell. The fluid–structure interaction effects are calculated in terms of generalized added masses, using a boundary integral equation method together with the method of images in order to impose an appropriate boundary condition on the free surface. To assess the influence of the contained and/or surrounding fluid on the dynamic behaviour of the shell structure, the wet natural frequencies and associated mode shapes were calculated and compared with available experimental measurements.

© 2002 Elsevier Science Ltd. All rights reserved.

1. INTRODUCTION

Dynamic characteristics of cylindrical shells partially or completely in contact with fluid are of great importance in a variety of engineering applications, such as, vibration of liquid storage tanks, flexible pipelines conveying fluid, etc. All these vibration problems are complicated by the interactions that take place between structure and fluid. This is due to the vibration of the structural surface in contact with the fluid medium imparting motion to the fluid, thus altering its pressure, and, hence, inducing reactive forces on its surface.

The free vibration analysis of partially filled, vertical cylindrical shells has been dealt with by various authors (see, for example, references [1–6]). However, only a few studies appear to have been carried out on the vibration of partially filled and submerged horizontal cylindrical shells. Amabili and Dalpiaz [7] investigated experimentally the natural frequencies and mode shapes of a partially filled horizontal cylindrical shell. Amabili [8] introduced two approximate analytical solutions to calculate the free vibration characteristics of a horizontal cylindrical shell when partially filled, and compared these

predictions with experimental measurements. Amabili [9] extended this study to investigate the effects of both internal and external fluid on dynamic characteristics. Alternatively, Ergin [10, 11] presented an approximate analytical method to calculate the natural frequencies and mode shapes of partially filled and submerged shells. In these studies [10, 11], although the velocity potential function adopted does not satisfy an appropriate boundary condition on the fluid's free surface, very good agreement was obtained with experimental measurements available in the open literature. In the same vein, Ergin *et al.* [12] studied the dynamic behaviour of a thin, horizontal cylindrical shell vibrating at fixed positions below a free surface in water of finite depths. In their analysis they calculated the generalized fluid loadings to assess the influence of free surface, rigid boundary and position of submerged cylinder on the dynamic characteristics of the shell structure.

In this paper, the dynamic characteristics (i.e., wet natural frequencies and mode shapes) of a partially filled and/or submerged, horizontal cylindrical shell are studied. In this investigation, it is assumed that the fluid is ideal, i.e., inviscid, incompressible and its motion is irrotational. Furthermore, the fluid forces are associated with the inertial effect of the fluid, i.e., the fluid pressure on the wetted surface of the structure is in phase with the structural acceleration. In the analysis, it is assumed that the empty shell vibrates in its *in vacuo* eigenmodes when it is in contact with fluid, and that each mode gives rise to a corresponding surface pressure distribution on the wet part of the structure. The *in vacuo* dynamic analysis entails the vibration of the shell in the absence of any external force and structural damping and the corresponding dynamic characteristics (e.g., natural frequencies and principal mode shapes) of the shell structure were obtained by using a standard finite element software (i.e., ANSYS [13]). At the fluid–structure interface, continuity considerations require that the normal velocity of the fluid is equal to that of the structure. The normal velocities on the wetted surface are expressed in terms of modal structural displacements, obtained from the *in vacuo* dynamic analysis. By using a boundary integral equation method the fluid pressure is eliminated from the problem, and using the method of images (i.e., imposing an appropriate free surface boundary condition), the fluid–structure interaction forces are calculated solely in terms of generalized added mass coefficients. During this analysis, the wet surface is idealized by using appropriate boundary elements, referred to as hydrodynamic panels. The generalized structural mass matrix is merged with the generalized added mass matrix and then the total generalized mass matrix is used in solving the eigenvalue problem for the partially filled and/or submerged structure. To assess the influence of the contained and surrounding fluid on the dynamic behaviour of the shell structure, the wet natural frequencies and associated mode shapes are calculated. A comparison of the predicted dynamic characteristics with available experimental measurement [8] shows very good agreement. In addition, for the half-submerged empty horizontal cylindrical shell (i.e., floating at a draught equal to its radius), the wet natural frequencies and associated mode shapes predicted by the current method compare very well with those obtained by using the three-dimensional hydroelasticity theory [12, 14].

2. MATHEMATICAL MODEL

2.1. GENERALISED EQUATION OF MOTION

The equation of motion describing the response of a flexible structure to external excitation may be written as [15]

$$\mathbf{M}\ddot{\mathbf{U}} + \mathbf{C}_v\dot{\mathbf{U}} + \mathbf{K}\mathbf{U} = \mathbf{P}, \quad (1)$$

where \mathbf{M} , \mathbf{C}_v , \mathbf{K} denote the mass, structural damping and stiffness matrices respectively. The vectors \mathbf{U} , $\dot{\mathbf{U}}$ and $\ddot{\mathbf{U}}$ represent the structural displacements, velocities and accelerations, respectively, and the column vector \mathbf{P} denotes the external forces.

In an *in vacuo* analysis, the structure is assumed to vibrate in the absence of any structural damping and external forces reducing equation (1) to the form

$$\mathbf{M}\ddot{\mathbf{U}} + \mathbf{K}\mathbf{U} = \mathbf{0}. \quad (2)$$

The form of equation (2) suggests that one can express the trial solution as

$$\mathbf{U} = \mathbf{D}e^{i\omega t}. \quad (3)$$

Using equation (3) in equation (2) and cancelling the common factor $e^{i\omega t}$, one obtains the equation

$$(-\omega^2\mathbf{M} + \mathbf{K})\mathbf{D} = \mathbf{0}. \quad (4)$$

This equation describes the simple harmonic oscillations of the free undamped structure and the *in vacuo* principle modes and natural frequencies are determined from the associated eigenvalue problem.

The distortions of the structure may be expressed as the sum of the distortions in the principal modes,

$$\mathbf{U} = \mathbf{D}\mathbf{p}(t) \quad (5)$$

where \mathbf{D} is the modal matrix whose columns are the *in vacuo*, undamped mode vectors of the structure. \mathbf{p} is the principal co-ordinates matrix. By substituting equation (5) into equation (1) and pre-multiplying by \mathbf{D}^T , the following generalized equation in terms of the principal co-ordinates of the structure is obtained [14]:

$$\mathbf{a}\ddot{\mathbf{p}}(t) + \mathbf{b}\dot{\mathbf{p}}(t) + \mathbf{c}\mathbf{p}(t) = \mathbf{Q}(t). \quad (6)$$

Here \mathbf{a} , \mathbf{b} , \mathbf{c} denote the generalized mass, damping and stiffness matrices, respectively, and are defined as follows:

$$\mathbf{a} = \mathbf{D}^T\mathbf{M}\mathbf{D}, \quad \mathbf{b} = \mathbf{D}^T\mathbf{C}_v\mathbf{D}, \quad \mathbf{c} = \mathbf{D}^T\mathbf{K}\mathbf{D}, \quad \mathbf{Q} = \mathbf{D}^T\mathbf{P}. \quad (7)$$

The generalized force matrix, $\mathbf{Q}(t)$ represents the fluid-structure interaction, $\mathbf{Z}(t)$, and all other external forces, $\mathbf{\Xi}(t)$.

2.2. FORMULATION OF THE FLUID PROBLEM

In the mathematical model, the fluid is assumed ideal, i.e., inviscid and incompressible, and its motion is irrotational and there exists a fluid velocity vector, \mathbf{v} , which can be defined as the gradient of the velocity potential function Φ as

$$\mathbf{v}(x, y, z, t) = \nabla\Phi(x, y, z, t), \quad (8)$$

where

$$\Phi(x, y, z, t) = \text{Re}[i\omega\phi(x, y, z)e^{i\omega t}] \quad (9)$$

and $\phi(x, y, z)$ satisfies Laplace's equation

$$\nabla^2\phi(x, y, z) = 0 \quad (10)$$

throughout the fluid domain.

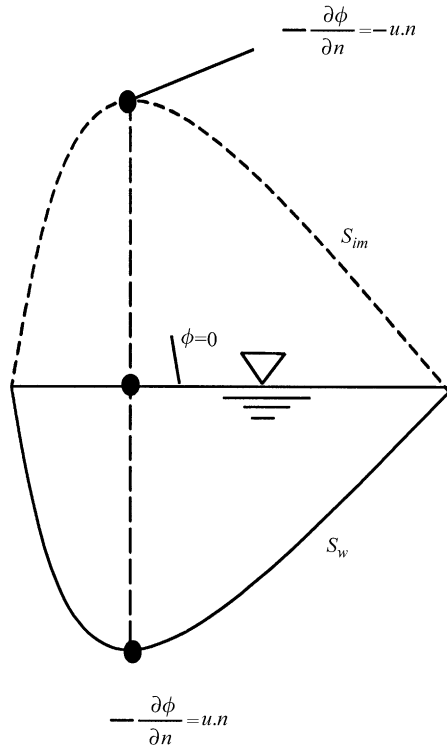


Figure 1. Wetted surface and image boundary for a partially filled structure.

On the wetted surface of the vibrating structure the fluid normal velocity must be equal to the normal velocity on the structure and this condition can be expressed as

$$\frac{\partial \phi}{\partial \mathbf{n}} = -\mathbf{u} \cdot \mathbf{n}, \tag{11}$$

where \mathbf{u} is the displacement vector of the median surface of the structure and \mathbf{n} is the unit normal vector on the wetted surface and points into the region of interest.

In this study, it is assumed that the structure vibrates at relatively high frequencies so that the effect of surface waves, for the partially filled and/or submerged shell, can be neglected. Therefore, the free surface condition for ϕ can be approximated by

$$\phi = 0 \tag{12}$$

on the free surface.

The method of images [16] may be used, as shown in Figure 1, to satisfy this condition. By adding an imaginary boundary region, the condition given by equation (12) at the horizontal free surface can be omitted; thus, the problem is reduced to a classical Neumann’s case. It should also be noted that, for the internal fluid, the normal fluid velocity cannot be arbitrarily specified. It has to satisfy the incompressibility condition

$$\iint_{S_w + S_{im}} \frac{\partial \phi}{\partial n} dS = 0, \tag{13}$$

where S_w and S_{im} represent the wetted and imaginary surfaces respectively (see Figure 1).

Exact solution of Laplace's equation (10) can be obtained for only a limited number of cases. An alternative solution method must be employed for a general type structure and domain. In the present study, a boundary integral equation method [17, 18] is applied in order to evaluate the fluid-structure interaction forces. The disturbance potential ϕ at some point (x, y, z) in a three-dimensional inviscid flow field due to an oscillating body can be expressed by means of a distribution of sources over the wetted and imaginary surfaces of the structure in the following form [18]:

$$\phi(x, y, z) = \iint_{S_w + S_{im}} \frac{1}{r(x, y, z; \xi, \eta, \zeta)} \sigma(\xi, \eta, \zeta) dS(\xi, \eta, \zeta), \quad (14)$$

where $r = [(x - \xi)^2 + (y - \eta)^2 + (z - \zeta)^2]^{1/2}$ and (ξ, η, ζ) and $\sigma(\xi, \eta, \zeta)$ denote a point and the unknown source distribution over the wetted and imaginary surfaces of the structure respectively.

By substituting boundary condition (11) into equation (14), the following integral equation is obtained for the source density distribution σ :

$$2\pi\sigma(x, y, z) - \iint_{S_w + S_{im}} \frac{\partial}{\partial \mathbf{n}} \left(\frac{1}{r(x, y, z; \xi, \eta, \zeta)} \right) \sigma(\xi, \eta, \zeta) dS(\xi, \eta, \zeta) = \mathbf{u}(x, y, z) \cdot \mathbf{n}(x, y, z). \quad (15)$$

Integral equation (15) is a two-dimensional Fredholm equation of the second kind. The continuous formulation of the solution indicates that equation (15) is to be satisfied at all points on the wetted and imaginary surfaces of the body. Numerically, it can be solved with the subdivision of the wetted and imaginary surfaces of the body into \bar{N} quadrilateral panels of area ΔS_j ($j = 1, 2, \dots, \bar{N}$) with the source strength, σ taken as constant over each panel. The discretized numerical solution of equation (15) is therefore satisfied only at chosen control points and these control points may be taken as the centroids of each panel. Therefore, the surface integral in equation (15) can be written as the sum of the integral over \bar{N} quadrilateral panels of area ΔS_j . Equation (15) now takes the form

$$2\pi\sigma_i - \sum_{j=1}^{\bar{N}} \alpha_{ij}\sigma_j = u_{ni} \quad (i = 1, 2, \dots, \bar{N}), \quad (16)$$

where

$$\alpha_{ij} = \iint_{\Delta S_j} \frac{\partial}{\partial \mathbf{n}} \left(\frac{1}{r(x_i, y_i, z_i; \xi, \eta, \zeta)} \right) dS \quad (17)$$

and u_{ni} represents the displacement in the direction of the normal at the control point of the i th panel. Thus, the influence coefficient α_{ij} may be thought of as representing the velocity induced at the i th control point (in the direction normal to the surface) by a source of unit strength distributed uniformly over the j th panel. It is assumed that all u_{ni} values are known *a priori* (obtained from the *in vacuo* analysis) and, therefore, the corresponding unknown source strength, σ_i , can be obtained from the solution of equation (16) for each principal mode shape.

2.3. GENERALIZED FLUID-STRUCTURE INTERACTION FORCES

Once the deformation potentials ϕ_k due to the oscillation of the body in its *in vacuo* eigenmodes are obtained, the r th component of the generalized fluid-structure interaction

force amplitude due to the k th modal vibration can be expressed in terms of pressure acting on the wetted surface of the structure as

$$\bar{Z}_{rk} = \iint_{S_w} \mathbf{n} \mathbf{u}_r \bar{p}_k \, dS, \tag{18}$$

where \mathbf{u}_r represents the r th *in vacuo* modal displacement vector. It should be noted that only the normal generalized force is considered since the tangential force exerted by the fluid is zero.

Upon the Bernoulli’s equation and neglecting the second order terms, the dynamic fluid pressure on the mean wetted surface of the flexible structure due to the k th modal vibration becomes

$$P_k = \text{Re}[\bar{p}_k e^{i\omega t}] = -\rho \frac{\partial \Phi_k}{\partial t}. \tag{19}$$

By substituting equation (9) into equation (19), the following expression for the pressure is obtained:

$$\bar{p}_k = \omega^2 \rho \phi_k. \tag{20}$$

The r th component of the generalized fluid–structure interaction force amplitude due to the k th modal vibration then takes the form

$$\bar{Z}_{rk} = \iint_{S_w} \mathbf{n} \mathbf{u}_r (\omega^2 \rho \phi_k) \, dS. \tag{21}$$

Therefore, the generalized added mass term can be defined as

$$A_{rk} = \frac{\rho}{\omega^2} \iint_{S_w} \mathbf{n} \mathbf{u}_r \omega^2 \phi_k \, dS. \tag{22}$$

If the k th principal co-ordinate is in the form of $p_k(t) = p_k e^{i\omega t}$, then the r th component of the generalized fluid–structure interaction force due to the k th response of the structure becomes [12]

$$\begin{aligned} Z_{rk}(t) &= \omega^2 A_{rk} p_k e^{i\omega t} \\ &= -A_{rk} \ddot{p}_k(t). \end{aligned} \tag{23}$$

2.4. CALCULATIONS OF WET FREQUENCIES AND MODE SHAPES

If it is assumed that the structure vibrates freely in the absence of damping and external excitation force, $\Xi(t)$, and that the fluid has negligible stiffness, the solution of the generalized equation of motion (6) may be expressed in the form of $\mathbf{p}(t) = \mathbf{p}_0 e^{i\omega t}$. Therefore, equation (6) is reduced to the form

$$[-\omega^2(\mathbf{a} + \mathbf{A}) + \mathbf{c}]\mathbf{p}_0 = \mathbf{0}. \tag{24}$$

By solving the eigenvalue problem, expressed by equation (24), the uncoupled modes and associated frequencies of the shell in contact with fluid are obtained. To each wet natural

frequency ω_r , there is a corresponding wet eigenvector $\mathbf{p}_{0r} = \{p_{r1}, p_{r2}, p_{r3}, \dots, p_{rM}\}$ satisfying equation (24). The corresponding uncoupled mode shapes for the cylinder in contact with internal and/or external fluid are obtained as [19]

$$\bar{\mathbf{u}}_r(\mathbf{x}, \mathbf{y}, \mathbf{z}) = \{\bar{u}_r, \bar{v}_r, \bar{w}_r\} = \sum_{j=1}^M \mathbf{u}_j(x, y, z) \mathbf{p}_{rj}, \quad (25)$$

where $\mathbf{u}_j(x, y, z) = \{u_r, v_r, w_r\}$ denote the *in vacuo* principal mode shapes of the empty horizontal cylindrical shell and M is the number of mode shapes included in the analysis. It should be noted that the hydrodynamic forces associated with the inertial effect of the fluid do not have the same spatial distribution as those of the *in vacuo* modal forms. Consequently, this produces hydrodynamic coupling between the modes. This coupling effect is introduced into equation (24) through the added mass matrix \mathbf{A} .

3. NUMERICAL RESULTS AND COMPARISONS

3.1. CONVERGENCE TESTS FOR FINITE ELEMENT AND BOUNDARY ELEMENT MESH SIZE

A horizontal circular cylindrical shell is chosen to demonstrate the applicability of the aforementioned theory to structures partially filled and/or submerged such as liquid storage tanks, submarine pressure hull, etc. The shell is of length $L = 664$ mm, radius $R = 175$ mm, and thickness $h = 1$ mm, made of stainless steel and sealed by steel plates at both ends. The shell was investigated experimentally by Amabili and Dalpiaz [7] and Amabili [8]. The *in vacuo* dynamic characteristics of this shell structure were obtained using the ANSYS finite element software [13]. This produces information on natural frequencies and principal mode shapes of the empty structure *in vacuo*. In these calculations, the thin cylindrical shell was discretized with four-noded quadrilateral shell elements, including both membrane and bending stiffness influences. However, a limited number of three-noded triangular elements were used to model the end seals.

In a preliminary calculation, 256 elements were distributed over the shell structure and 48 elements over each end. The distribution over the cylindrical shell consists of 16 equally spaced elements around the circumference and 16 equally spaced elements along the shell structure. To test the convergence of the calculated dynamic properties, i.e., natural frequencies and principal mode shapes, the number of elements over the cylindrical shell surface was increased first to 1024—32 elements around the circumference and 32 elements along the shell and to 96 over each end. Finally, the number of elements around the circumference was increased to 64 whilst the number of elements along the shell was retained as 32. Therefore, a total number of 2432 elements were distributed over the whole structure with 192 elements over each end seal. Table 1 shows the calculated natural frequencies obtained from the analytical calculations, based on the assumption of simply supported end conditions, [10, 20] and ANSYS for the first eight modes. The results occur in pairs. That is, in general, for each natural frequency, there exists a pair of mode shapes satisfying the relevant orthogonality conditions. The mode shapes of the shell structure *in vacuo* are identified with the number of standing waves around the circumference, n , and the number of half-waves along the shell, m . It should be noted that the circumferential number of standing waves does not necessarily occur in order of sequence, as can be seen from Table 1. The order depends on geometrical characteristics of the shell structure. The *in vacuo* dynamic characteristics of the shell are scaled to a generalized mass of 1 kg m^2 . The differences in the results, shown in Table 1, indicate that the calculated values are slowly converging with increasing number of elements. The results of the final idealization (2432

TABLE 1

Convergence of FEM natural frequencies (in vacuo) (Hz)

Mode (<i>m, n</i>)	16 × 16 idealization	32 × 32 idealization	64 × 32 idealization	Analytical [10, 20]
1-4	226.2	223.8	223.8	221.1
1-4	227.4	225.0	224.2	
1-5	241.6	234.1	232.4	230.3
1-5	241.6	234.1	232.4	
1-6	319.2	303.1	299.2	298.0
1-6	319.2	303.3	299.2	
1-3	316.4	317.1	317.1	315.7
1-3	316.4	317.1	317.1	

TABLE 2

Convergence of wet natural frequencies for the half-filled cylindrical shell (Hz)

Mode	16 × 32 idealization	32 × 32 idealization	32 × 64 idealization
1	109.0	101.2	101.1
2	110.2	102.0	102.0
3	140.9	130.5	130.3
4	145.6	134.5	134.4
5	197.2	184.6	184.4
6	202.8	186.6	186.5

elements) compare very well with the analytical calculations; hence, they were adopted for the *in vacuo* dynamic characteristics of the horizontal cylindrical shell.

To test the convergence of the hydrodynamic predictions, various numbers of hydrodynamic panels were distributed around the circumference and along the length of the wetted surface for the half-filled cylindrical shell. The main aim of this exercise was to represent accurately the distortional mode shapes of the wetted surface area of the structure. For the half-filled shell, three different idealizations of panel distribution over the wetted surface of the cylindrical structure were considered (see Table 2). In the first idealization, the distribution involved 16 equally spaced quadratic panels around the wetted circumference and 32 equally spaced quadratic panels along the cylindrical shell. Thus, a total number of 512 panels were adopted over the wetted surface of the shell. In a second idealization, 1024 panels were used—the number of panels around the wetted circumference was increased to 32, whilst the distribution along the shell was maintained as in the first idealization. Finally, for a third idealization, the number of panels along the shell structure was increased to 64 whilst the number of panels distributed around the wetted shell circumference was retained as 32. Therefore, a total number of 2048 panels were adopted over the wetted surface of the shell structure for this final idealization. Table 2 shows the convergence of the predicted wet natural frequency values with increasing number of hydrodynamic panels for the half-filled cylindrical shell. The discrepancies between the predictions based on the 32 × 32 and 32 × 64 idealizations are negligibly small for the first six wet modes of the half-filled cylindrical shell. Therefore, it can be concluded that the 32 × 32 idealization adequately represents the distortional shapes around the circumference and along the shell. The same angular

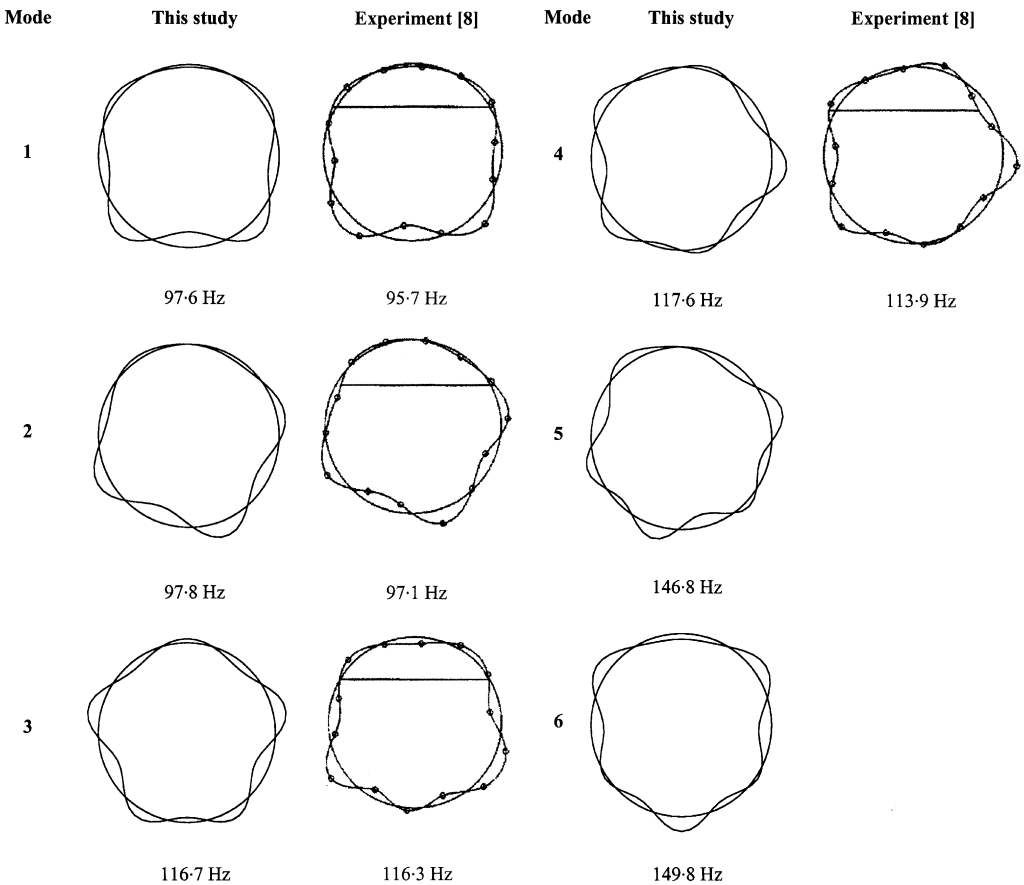


Figure 2. Modes and associated frequencies of 4/5 filled cylindrical shell.

(approximately 5.63°) and axial spaces (2.075 cm) were also adopted for the results presented in Figures 2–5 and Tables 3 and 4(a) and (b). Accordingly, the wetted surface of the cylindrical shell was discretized using 1024 hydrodynamic panels for the half-filled and/or half-submerged cases—32 around the wetted circumference and 32 along the shell, and 1344 hydrodynamic panels for the 4/5-filled case—42 around the wetted circumference and 32 along the shell and 704 hydrodynamic panels—22 around the wetted circumference and 32 along the shell for the 1/5-filled case. In addition, for the partially filled and/or submerged shell structure, convergence studies were carried out to establish the number of modes needed for the predictions presented in this study. A maximum number of $M = 24$ *in vacuo* modes was included in the analysis—12 of which were symmetric and 12 antisymmetric with respect to the symmetry plane through the centre of the shell and perpendicular to the free surface of the fluid.

3.2. CALCULATED RESULTS AND COMPARISONS

By solving the eigenvalue problem, equation (24), the uncoupled modes and associated frequencies of the shell partially in contact with fluid are obtained. Figures 2, 3 and 4 show the predicted mode shapes and wet natural frequencies, respectively, for the 4/5-filled,

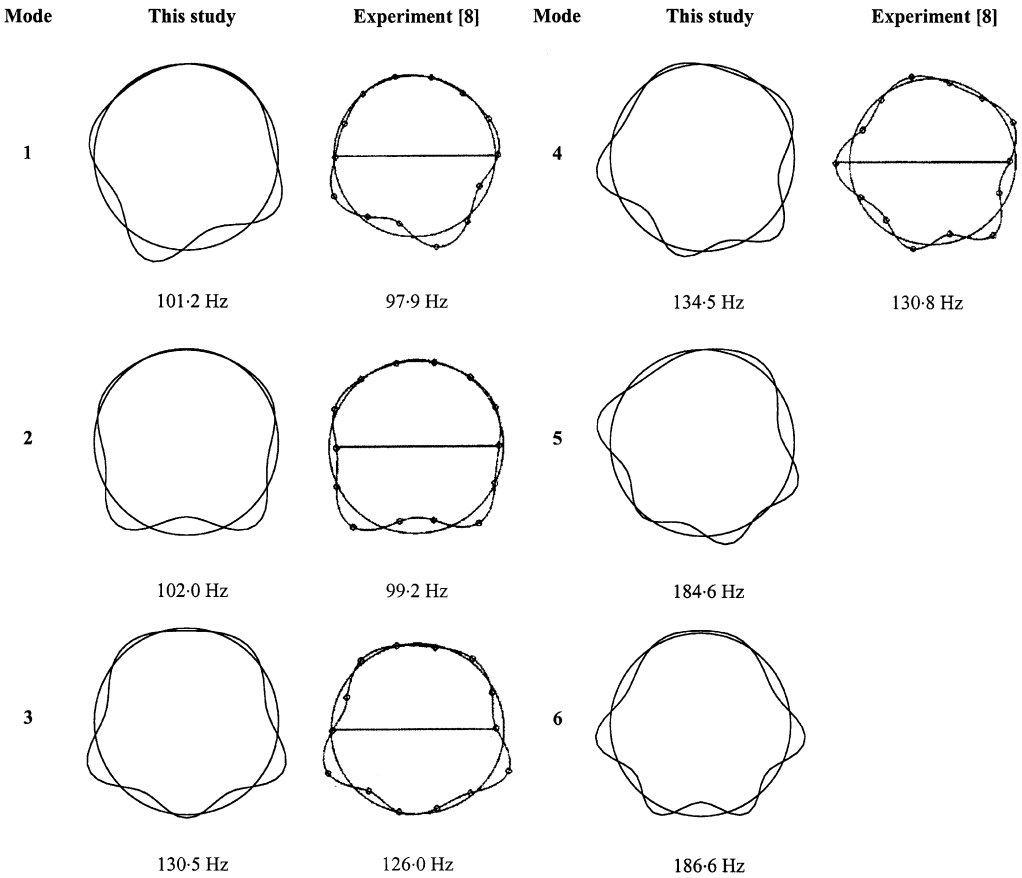


Figure 3. Modes and associated frequencies of half filled cylindrical shell.

half-filled and 1/5-filled shells. It must be realized that the mode shapes are either symmetric or antisymmetric about the plane through the centre of the shell and perpendicular to the free surface of the fluid. The mode shapes in Figures 2–4, corresponding to the first six wet natural frequencies, are ordered and numbered simply with frequency increasing; because of this, the circumferential mode shapes are not described by the circumferential wave patterns as obtained from the *in vacuo* analysis. All the modes shown in Figures 2–4 have a shape with one longitudinal half-wave ($m = 1$). The predicted wet natural frequencies and mode shapes, obtained from equations (24) and (25), respectively, compare very well with the corresponding experimental results [8], as seen in Figures 2–4. However, there are differences between the predictions and experimental measurements. These differences lie in the range between 0.3 and 3.2% for the 4/5-filled cylinder, 2.8 and 3.5% for the half-filled cylinder, and 0.2 and 3.2% for the 1/5-filled cylinder. The wet natural frequencies for the partially filled horizontal cylindrical shell are summarized in Table 4(a).

The generalized added mass values associated with the distortional *in vacuo* modes are a function of the number of waves around the circumference and the number of half-waves along the cylinder. They gradually decrease with increasing number of circumferential waves, n . The calculated generalized added mass values, for only the half-filled shell structure, are presented in Table 3 for the first 10 distortional mode shapes—five symmetric and five antisymmetric. Table 3 also shows the hydrodynamic coupling between the

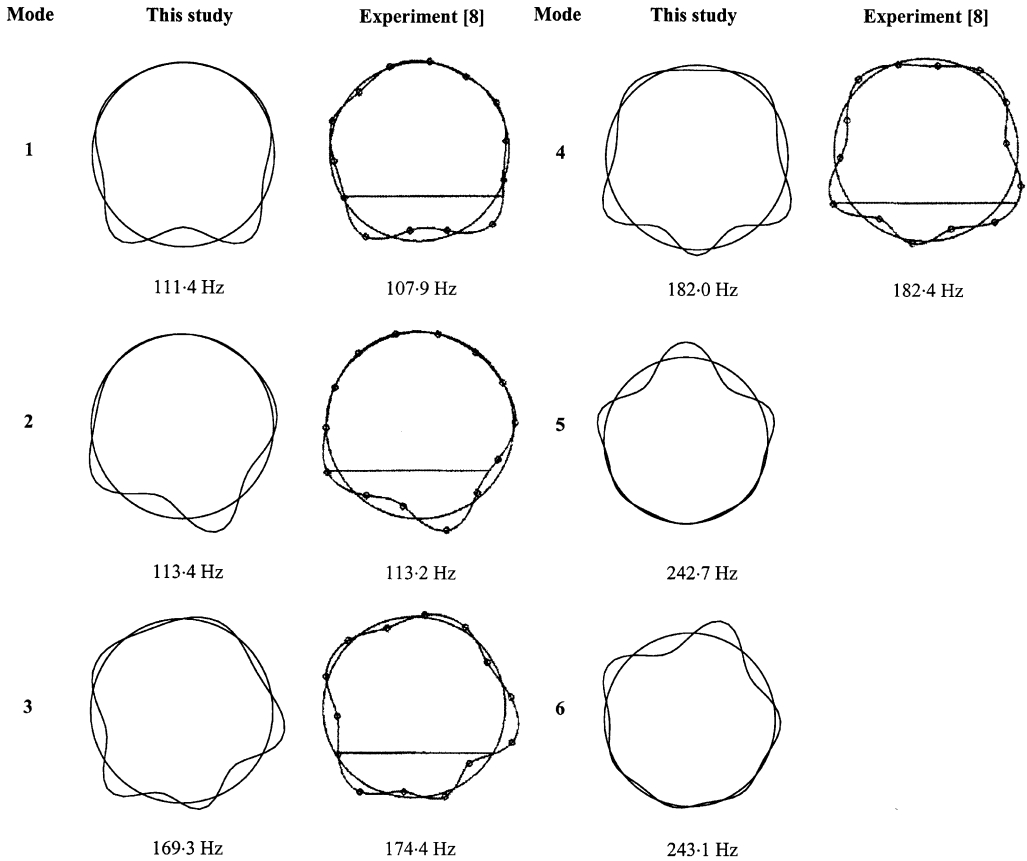


Figure 4. Modes and associated frequencies of 1/5 filled cylindrical shell.

in vacuo mode shapes. It is expected that the hydrodynamic coupling between the symmetric and antisymmetric modes would be very small. However, there is considerable coupling between some symmetric and antisymmetric modes. This is because some of the mode shapes obtained from the finite element analysis are not perfectly symmetric or antisymmetric with respect to the plane of symmetry. The generalized added mass values in Table 3 are obtained for the *in vacuo* modes scaled to a generalized mass of 1 kg m^2 .

The analysis was subsequently extended to investigate the effect of the external fluid on the dynamic behaviour of the empty shell. The calculated wet natural frequencies and associated mode shapes are shown in Figure 5 for the cylindrical shell half-submerged (i.e., floating at a draught equal to its radius). All wet natural frequencies and associated mode shapes shown in Figure 5 are evaluated by using equations (24) and (25) respectively. The predictions for the current method make use of equation (22) when calculating the generalized added mass matrix \mathbf{A} . The values of the current method compare well with those obtained from the three-dimensional hydroelasticity method [12], as can be seen in Figure 5. The hydroelasticity method includes the influence of the boundary constraints introduced by the free-surface disturbances. Therefore, in order to obtain a frequency-independent generalized added mass for the half-submerged shell, a very high frequency of oscillation (i.e., 100 rad/s) on the free surface is considered. It is well known that, for a surface-piercing oscillating body or a submerged body oscillating close to the free

TABLE 3

Generalized added mass coefficients (kg m²) of the half-filled cylindrical shell for the first ten modes

Mode <i>m, n</i>	1, 4 sym	1, 4 asym	1, 5 sym	1, 5 asym	1, 6 sym	1, 6 asym	1, 3 sym	1, 3 asym	1, 7 sym	1, 7 asym
1, 4 sym	2.22	0.0	1.34	0.43	-0.15	0.0	1.74	0.0	-0.26	-0.28
1, 4 asym	0.0	2.46	-0.43	1.32	0.0	0.0	0.0	1.77	0.27	-0.25
1, 5 sym	1.34	-0.43	1.97	0.05	-1.08	-0.35	0.0	0.0	0.0	0.0
1, 5 asym	-0.43	1.32	0.05	1.83	-0.35	1.09	0.0	0.24	-0.07	0.07
1, 6 sym	-0.15	0.0	-1.07	-0.35	1.52	0.0	0.45	0.0	-0.65	-0.69
1, 6 asym	0.0	0.0	-0.35	1.09	0.0	1.63	0.0	-0.46	-0.69	0.64
1, 3 sym	1.74	0.0	0.0	0.0	0.45	0.0	3.15	0.0	0.0	0.0
1, 3 asym	0.0	1.77	0.0	0.24	0.0	-0.46	0.0	2.70	0.12	-0.11
1, 7 sym	-0.26	0.27	0.02	-0.07	-0.65	-0.68	0.0	0.12	1.32	0.04
1, 7 asym	-0.28	-0.25	0.0	0.07	-0.69	0.64	0.0	-0.11	0.04	1.33

TABLE 4

Predicted wet natural frequencies of partially filled cylindrical shell (Hz) (a) and Partially filled and half-submerged cylindrical shell (Hz) (b)

(a)				
Mode	4/5-filled	1/2-filled	1/5-filled	Empty
1	97.6	101.2	111.4	223.8
2	97.8	102.0	113.4	224.2
3	116.7	130.5	169.3	232.4
4	117.6	134.5	182.0	232.4
5	146.8	184.6	242.7	299.2
6	149.8	186.6	243.1	299.2

(b)				
Mode	4/5-filled half-submerged	1/2-filled half-submerged	1/5-filled half-submerged	Empty half-submerged
1	73.5	74.6	79.0	99.9
2	73.9	75.3	79.4	100.8
3	92.3	97.2	113.5	129.1
4	94.3	100.8	115.1	133.1
5	123.2	140.9	164.4	184.1
6	126.4	143.3	169.7	185.1

surface, the generalized hydrodynamic forces exhibit frequency dependence because of the free surface wave disturbances. The generalized added mass values start with large finite values at very small frequencies, increase to their maximum values in the low-frequency region, and decrease in value until they reach a constant value at higher frequencies [12]. Therefore, these constant generalized added mass values were used for the results of the three-dimensional hydroelasticity method presented in Figure 5.

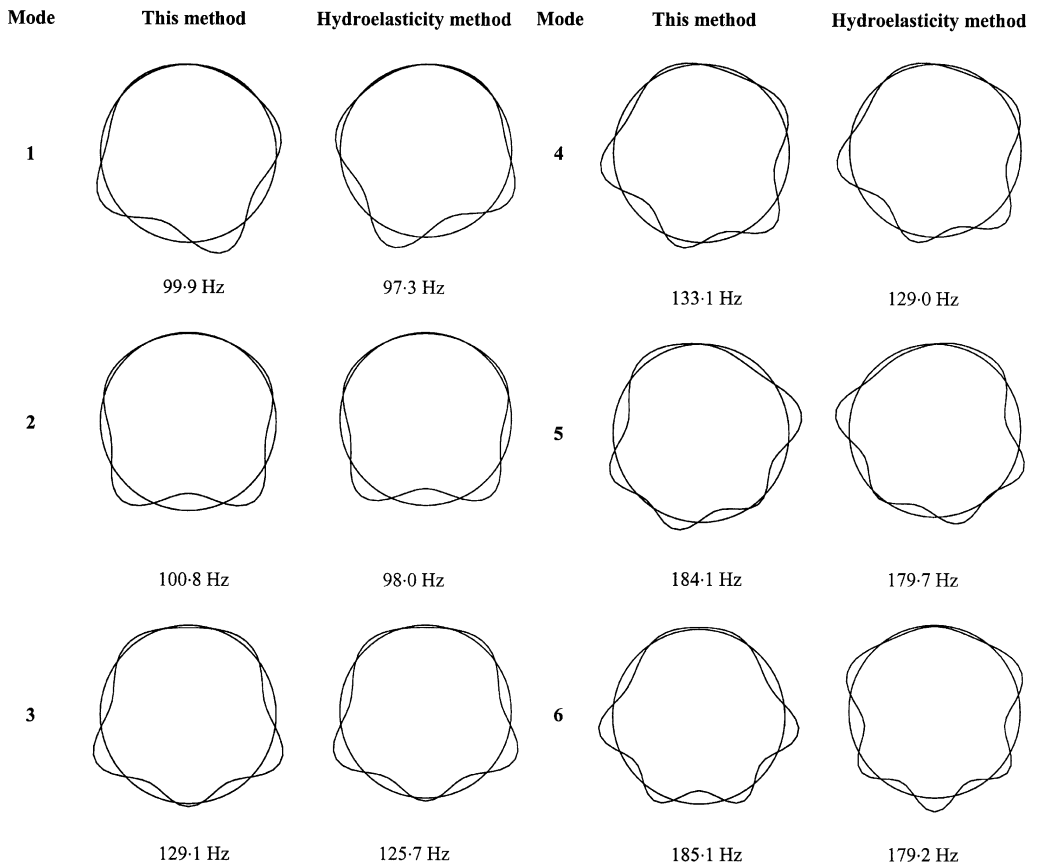


Figure 5. Modes and associated frequencies of half submerged cylindrical shell.

In a further study, the effect of both external and contained fluids on the dynamic behaviour of the shell structure was investigated. The calculated wet natural frequencies are presented in Table 4(b) for the cases of the empty, half-filled, 4/5-filled and 1/5-filled, half-submerged horizontal cylindrical shells. The same panel idealization used for the half-filled cylindrical shell was adopted for the outer wetted surface of the half-submerged shell in all cases. The wet natural frequency values behave as expected. That is to say that these frequencies decrease with increasing area of contact with the fluid. The largest area of contact was in the case of the 4/5-filled and half-submerged shell. Therefore, the lowest frequencies occurred in this case (see Table 4(b)). It should be noted that all the cases where this cylindrical shell is floating are artificial in the sense that the shell is not free-floating.

4. CONCLUSIONS

Free vibration characteristics of partially filled and/or submerged horizontal cylindrical shells were obtained through an approach based on a boundary integral equation and the method of images which is demonstrated to be suitable for relatively high-frequency structures. The *in vacuo* dynamic characteristics (i.e., natural frequencies and mode shapes) of the horizontal shell were obtained by using the finite element idealization of 64 elements around the circumference and 32 elements along the shell. A maximum number of 24

in vacuo modes—12 symmetric and 12 antisymmetric were calculated by using the ANSYS finite element software and they were included in the wet part of the analysis. For the hydrodynamic calculations, the 1024, 1344 and 704 hydrodynamic panel idealizations were adopted, respectively, for the half-filled and/or submerged, 4/5-filled and 1/5-filled shell cases.

From the results presented, the calculations based on the boundary integral equation method with the method of images show a good agreement with the experimental measurement [8] (see Figures 2–4). However, as seen from these figures, there appears a tendency to overestimate slightly the values of resonance frequencies. The differences lie within the limits that one would expect when comparing experimental results with numerical calculations. On the other hand, the results of the present study are also in good agreement with the predictions based on the three-dimensional hydroelasticity method [12]. This present study confirms that the theory described here is applicable to high-frequency structures such as liquid storage tanks, pipelines, etc.

As seen from the generalized added masses of Table 3, there is a considerable coupling between some of the symmetric and antisymmetric *in vacuo* modes. This is because some of the *in vacuo* modes are not perfectly symmetric or antisymmetric with respect to the symmetry plane that passes through the centre of the cylinder and is perpendicular to the free surface of the water. This matter requires further investigation. It can be also realized from Table 3 that the generalized added mass values decrease with increasing number of circumferential waves, n .

It can be seen from Tables 4(a) and (b) that the frequency values behave as expected. That is to say that the frequencies decrease with increasing area of contact with the fluid. The largest area of contact was in the case of 4/5-filled and half-submerged cylindrical shell. Therefore, the lowest frequencies occurred in this case. On the other hand, it should be noted that the calculated wet natural frequencies of the half-filled shell are quite similar to those of the empty, but half-submerged shell. As seen from Tables 4(a) and (b), the wet natural frequencies of the half-filled shell are slightly higher than those of the half-submerged and empty shell.

The present study has demonstrated the versatility of the method developed through a cylindrical shell with no internally attached structures. Future work, thus, may include the investigation of the dynamic characteristics of the shell structure with internal attachments such as ribs, struts, platforms, etc. The present method may also be extended to determine the effects of a flowing fluid on the vibration characteristics of an anisotropic cylindrical shell submerged and may be subjected to an internal and/or external flow.

ACKNOWLEDGMENTS

This research was supported by Istanbul Technical University (Project No. 842). One of the authors, A. Ergin, also greatly acknowledges the support from the Royal Society and the Scientific and Technical Research Council of Turkey during his two month's stay at Southampton University, England.

REFERENCES

1. A. A. LAKIS and M. P. PAÏDOUSSIS 1971 *Journal of Sound and Vibration* **19**, 1–15. Free vibration of cylindrical shells partially filled with liquid.
2. F. G. RAMMERSTORFER and K. SCHARF 1990 *Applied Mechanics Review* **43**, 261–282. Storage tanks under earthquake loading.

3. T. KOGA and M. TSUSHIMA 1990 *International Journal of Solids Structures* **26**, 1005–1015. Breathing vibrations of a liquid-filled circular cylindrical shell.
4. M. AMABILI, M. P. PAÏDOUSSIS and A. A. LAKIS 1998 *Journal of Sound and Vibration* **213**, 259–299. Vibrations of partially filled cylindrical tanks with ring-stiffeners and flexible bottom.
5. M. AMABILI 1999 *Journal of Sound and Vibration* **221**, 567–585. Vibrations of circular tubes and shells filled and partially immersed in dense fluids.
6. M. AMABILI 2000 *Journal of Sound and Vibration* **231**, 79–97. Eigenvalue problems for vibrating structures coupled with quiescent fluids with free surface.
7. M. AMABILI and G. DALPIAZ 1995 *Transactions of the American Society of Mechanical Engineers, Journal of Vibration and Acoustics* **117**, 187–191. Breathing vibrations of a horizontal circular cylindrical tank shell, partially filled with liquid.
8. M. AMABILI 1996 *Journal of Sound and Vibration* **191**, 757–780. Free vibration of partially filled, horizontal cylindrical shells.
9. M. AMABILI 1997 *Transactions of the American Society of Mechanical Engineers, Journal of Vibration and Acoustics* **119**, 476–484. Flexural vibration of cylindrical shells partially coupled with external and internal fluids.
10. A. ERGIN 1997 *Journal of Sound and Vibration* **207**, 761–767. An approximate method for the free vibration analysis of partially filled and submerged, horizontal cylindrical shells.
11. A. ERGIN 1997 *Proceedings of the 8th International Congress on Marine Technology, International Maritime Association of Mediterranean, Istanbul, Turkey, Section 2*, 21–30. Dynamic characteristics of partially filled and submerged cylindrical tanks.
12. A. ERGIN, W. G. PRICE, R. RANDALL and P. TEMAREL 1992 *Journal of Ship Research* **36**, 154–167. Dynamic characteristics of a submerged, flexible cylinder vibrating in finite water depths.
13. ANSYS, User's Manual, 1994.
14. R. E. D. BISHOP, W. G. PRICE and Y. WU 1986 *Philosophical Transactions of the Royal Society of London, Series A*, **316**, 375–426. A general linear hydroelasticity theory of floating structures moving in a seaway.
15. A. ERGIN 1997 *Computers and Structures* **62**, 1025–1034. The response behaviour of a submerged cylindrical shell using the doubly asymptotic approximation method (DAA).
16. F. KITO 1970 *Principles of Hydro-Elasticity*. Tokyo: Keio University.
17. J. L. HESS and A. M. O. SMITH 1967 in *Progress in Aeronautical Sciences* (D. Küchemann *et al.*, editors), Vol. **8**, 1–138. Calculation of potential flow about arbitrary bodies.
18. J. L. HESS 1975 *Computer Methods in Applied Mechanics and Engineering* **5**, 145–196. Review of integral-equation techniques for solving potential-flow problems with emphasis on the surface-source method.
19. R. E. D. BISHOP and W. G. PRICE 1979 *Hydroelasticity of Ships*. Cambridge: Cambridge University Press.
20. G. B. WARBURTON 1976 *The Dynamic Behaviour of Structures*. Oxford: Pergamon Press.